

---

# Variability of Hydroxyapatite-Coated Dental Implants

Karlis A. Gross, BE, M Eng Sci, PhD\*/Chris C. Berndt, PhD\*\*/Vincent J. Iacono, DMD\*\*\*

---

Uniformity, surface roughness, and chemical phase structure are all important features of implant coatings. While the first two variables are important for implant placement, the phase structure affects implant fixation. This study examined the coating morphology and the amount, size, and distribution of crystalline regions of press-fit and screw-type dental implants. Implants obtained from five commercial vendors were sectioned sagittally, mounted, and polished to reveal the coating microstructure. The crystalline phase content varied depending on the implant supplier; however, general trends were observed. Amorphous regions were predominantly found at the metal interface and decreased toward the outside of the coating, producing a crystallinity graded coating. The distal end of the implant, where heat build-up was more likely during the coating procedure, displayed a higher crystalline content and larger crystalline regions. Similarly, the thread apex consisted of more of a crystalline phase. The results of this study of coating microstructure may be used to improve the quality and performance of implants and may help to explain different in vivo responses to the many available varieties of hydroxyapatite-coated dental implants.

(INT J ORAL MAXILLOFAC IMPLANTS 1998;13:601-610)

**Key words:** coating microstructure, crystalline phase content, hydroxyapatite-coated dental implants

---

The implant system is very versatile and includes a range of sizes, shapes, coatings, and abutments.<sup>1</sup> Implant length can be chosen to fit the available bone and the abutment selected in a size and angle to accommodate the final restoration. Implant shape, which has received significant attention, is usually of a cylindrical press-fit or screw-type design. The selection of implant shape is determined by the available bone type and personal preference. A threaded implant provides immediate fixation but can only be placed where sufficient bone is available. The implant surface further affects the fixation and stabi-

lization of the implant. For example, a stepped cylinder such as the Tübingen<sup>2,3</sup> and screw-type implants have more surface for bonding compared to a press-fit implant. However, a porous coating on a cylinder can achieve more bone contact per implant length than a threaded design.<sup>4</sup> Other alternatives for surface modification of implants include a roughened surface, such as a grit-blasted titanium surface,<sup>5,6</sup> microgrooved or plasma-sprayed titanium,<sup>7</sup> and a plasma-sprayed hydroxyapatite coating.<sup>8</sup>

Hydroxyapatite coatings deposited by thermal spraying<sup>9</sup> have been used on dental implants<sup>10</sup> and orthopedic prostheses<sup>11</sup> for more than a decade. They have provided a rapid and stronger fixation to the surrounding bone in femoral implants.<sup>12</sup> In the dental application, the osteoconductive effect of hydroxyapatite has produced enhanced bone growth in type 3 and type 4 bone and could be a key factor in increasing implant fixation.<sup>13</sup> The utility of hydroxyapatite in the form of a coating is being investigated in situations that may find application in the clinical setting. Experimental studies on animals have shown that hydroxyapatite-coated implants may be used in fresh extraction sites<sup>14</sup> and immediately loaded applications.<sup>15</sup> The potential benefits of hydroxyapatite

---

\*Research Fellow, Department of Materials Engineering, Monash University, Clayton, Australia.

\*\*Professor, Department of Orthopaedics, State University of New York at Stony Brook, Stony Brook, New York.

\*\*\*Professor and Chair, Director, Advanced Education Program in Periodontics, Department of Periodontics, School of Dental Medicine, State University of New York at Stony Brook, Stony Brook, New York.

**Reprint requests:** Dr Karlis A. Gross, Department of Materials Engineering, Monash University, Clayton, Victoria 3168, Australia. Fax: (613) 9905-4940.

continue to fuel the impetus to improve both the coating performance and implant integration. Many commercial vendors and others offer numerous hydroxyapatite-coated implants from the selection of available implant shapes.

The advantages of hydroxyapatite are only useful if bonding is maintained at the metallic substrate-coating interface, the coating-bone interface, and within the coating. Coatings deposited on titanium sometimes have failed because of exfoliation,<sup>16</sup> delamination,<sup>17-19</sup> or release of coating segments.<sup>20,21</sup> These failures have stimulated an interest in examining the implants at a more detailed level.

In a fashion similar to machined titanium implants, which have undergone intense scrutiny,<sup>22,23</sup> hydroxyapatite coatings have also undergone examination, and findings indicate that they vary considerably among different vendors.<sup>24</sup> A study of the amorphous phase content in plasma-sprayed hydroxyapatite coatings on implants from different vendors revealed a range of 40 to 80 wt%<sup>25,26</sup> (Fig 1). In these studies, x-ray diffraction was conducted on the coating after it was removed from the implant and ground to a fine powder.

Presence of the amorphous phase has been reported in studies of hydroxyapatite-coated dental implants using x-ray diffraction. This information has provided the overall amorphous phase content when conducted on a powdered coating, or the composition to a depth of 10  $\mu\text{m}$  in the outside layer of the coating when examined *de novo* (with copper potassium alpha radiation) (unpublished data, 1997). However, analysis of the coating microstructure provides information that cannot be revealed in an x-ray diffraction pattern. Examination of the coating cross section is an important and accepted means of evaluating thermal-spray coatings. The location and size of the amorphous phase can be readily ascertained with light microscopy, and this information will provide an insight into the performance of the coating. In this paper, data are presented from a microscopic study of hydroxyapatite coatings, including the size, distribution, and location of the amorphous phase in coatings from different commercially available implants. Crystallinity in this article does not refer to nanocrystalline regions, but rather to clearly defined regions that do not include the crystalline phase.

## Materials and Methods

Screw-type and cylindrical implants with a hydroxyapatite coating were obtained from Dentsply (Encino, CA), Imtec (Ardmore, OK), Interpore (Irvine, CA), LifeCore (Chaska, MN), and Steri-Oss (Loma Linda, CA). These implants were fixed to a mounting block

with cyanoacrylate adhesive and cut sagittally using a diamond saw set at a low speed so as to minimize coating delamination. Lubrication during cutting ensured that wear debris were continuously removed from the freshly cut surface. Sectioning of each implant required a period of 30 to 40 minutes.

Sectioned implants were cleaned with ethanol and mounted in a slow-curing (24-hour) epoxy resin before metallographic polishing. Specimens were ground flat on 400-grit silicon carbon paper and progressively ground on 800- and 1000-grit papers before being polished with diamond paste. Final polishing with a 0.05- $\mu\text{m}$  alumina paste ensured preferential removal of the softer amorphous phase. This final stage was critical since excessive polishing produces a "more difficult to interpret" coating with less amorphous phase accompanied by a deeper topography.

Materials with a lower density, such as an amorphous phase, possess a smaller index of refraction. According to Fresnel's formula, the fraction of light reflected from a crystalline surface will be greater than that from an amorphous material surface of the same composition, based on the higher refractive index material of the more dense crystalline phase.<sup>27</sup> The crystalline phase will thus be brighter than the amorphous phase. Preferential removal of the amorphous phase on polishing will result in small, light-grey, raised plateaus in the microstructure, whereas the amorphous phase will be set lower and have a darker-grey appearance. The crystalline portion of the coating may consist of a small number of tricalcium phosphate, calcium oxide, and other phases, but the number of these phases should be small in a plasma-spray-coated implant<sup>28</sup> and thus does not distinguish it from hydroxyapatite. In the micrographs shown below, the metallic implant is identified by the white area located to the left, followed by the coating, and then the epoxy resin on the right.

The sagittal sections of the polished implant were examined in a light microscope at a magnification of 400 $\times$ . A small aperture was employed to decrease the spherical aberration and a Nomarski interference method to increase the depth of field and contrast of the features. The coating on each implant was carefully inspected and a section chosen to represent the typical features in that part of the implant. Microstructural analysis was then performed on three areas: at the top, middle, and distal locations, as shown in Fig 2. When a screw-type implant was analyzed, the threaded area was inspected to reveal the area at the apex and root of the thread. Crystallinity was determined by physically removing the crystalline areas from an image enlarged to four times the size and then determining the area fraction of this phase with respect to the entire coating area.

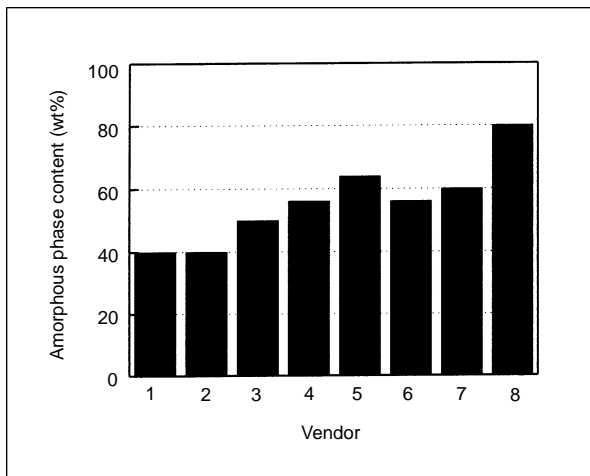


**Fig 1** Amorphous phase content of commercially available hydroxyapatite coatings (from studies by Krauser<sup>25</sup> and by Glick et al<sup>26</sup>).

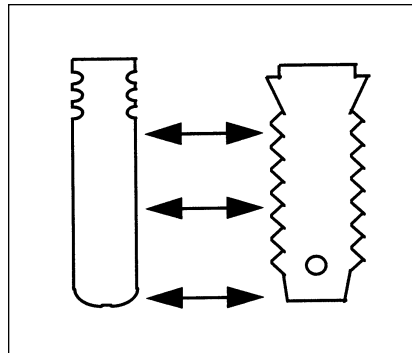


**Fig 2** Location of analysis for the cylindrical (*left*) and screw-type (*right*) implants.

This analysis was conducted only on several coating microstructures in which the crystalline phase was defined by large, easily located crystalline areas. The error in this measurement is 5%.

## Results

**Substrate Type, Coating Thickness, and Roughness.** Coatings have been deposited onto roughened or precoated implants. Roughening is typically achieved by grit-blasting to produce a surface with a roughness of less than 6  $\mu\text{m}$ . All of the implants were prepared in this manner except for one, a press-fit type of implant to which a metallic bond coat was applied since the external geometry is less important. The bond coat has some porosity (as noted by darker areas in Fig 3a), which is a controllable option in the thermal-spray process.

The combined effect of the bond coat and partially molten particles in the implant shown in Fig 3a have effectively produced a larger surface roughness compared to implants without these coating features.

The surface to be coated is also important for threaded designs. A rough surface preparation produced a change in the original thread shape (Fig 4d), although this did not occur for a similarly prepared implant, as shown in Fig 4b. The thread was very wide and shallow for this implant and the influence on the thread characteristics was therefore less pronounced.

Coating thickness is typically 50 to 100  $\mu\text{m}$  for dental implants, whereas the mean thickness, assessed at five different points on the coating cross section for the implants studied, varied from 30 to 75  $\mu\text{m}$ . Thickness was uniform around the implant; how-

ever, it tended to increase slightly toward the collar of the implant (Figs 3a, 3d, and 4a). This slight increase in thickness at the collar, while not intended in the design, would however provide a tighter interference fit with bone, preventing passage of fluid to the lower end of the implant.

The threaded implants displayed different thread types. The pitch and thread characteristics were different on each implant. Coating thickness on the threads was uniform in three cases, but in the fourth (Fig 4a), it showed nonuniformity on the thread. The root of the thread was preferentially filled, thus changing the apparent thread geometry of the implant.

**Coating Crystallinity.** A map (Fig 5) assists in the identification of the shape and position of the crystalline areas. The crystalline phase may appear (a) rounded, representing the core of a partially molten particle; (b) of lenticular shape, which is the core of a flattened molten droplet; (c) recrystallized in small isolated areas; and (d) crystalline in massive areas. Formation of these crystalline areas will be discussed later.

The titanium substrate is located to the left on each of the micrographs. An epoxy resin mounting material, used to hold the coating during specimen preparation, appears grey and may be difficult to distinguish from the amorphous phase at the outer surface of the coating in Figs 3a and 4a.

The amorphous phase is most easily seen in Fig 3a, where the large crystalline islands appear in an amorphous "sea." The white spot is part of the metallic bond coat. Coating crystallinity, or "the amount of crystalline phase" in the collar and middle of the implant was 40 to 50%. The majority of the crys-

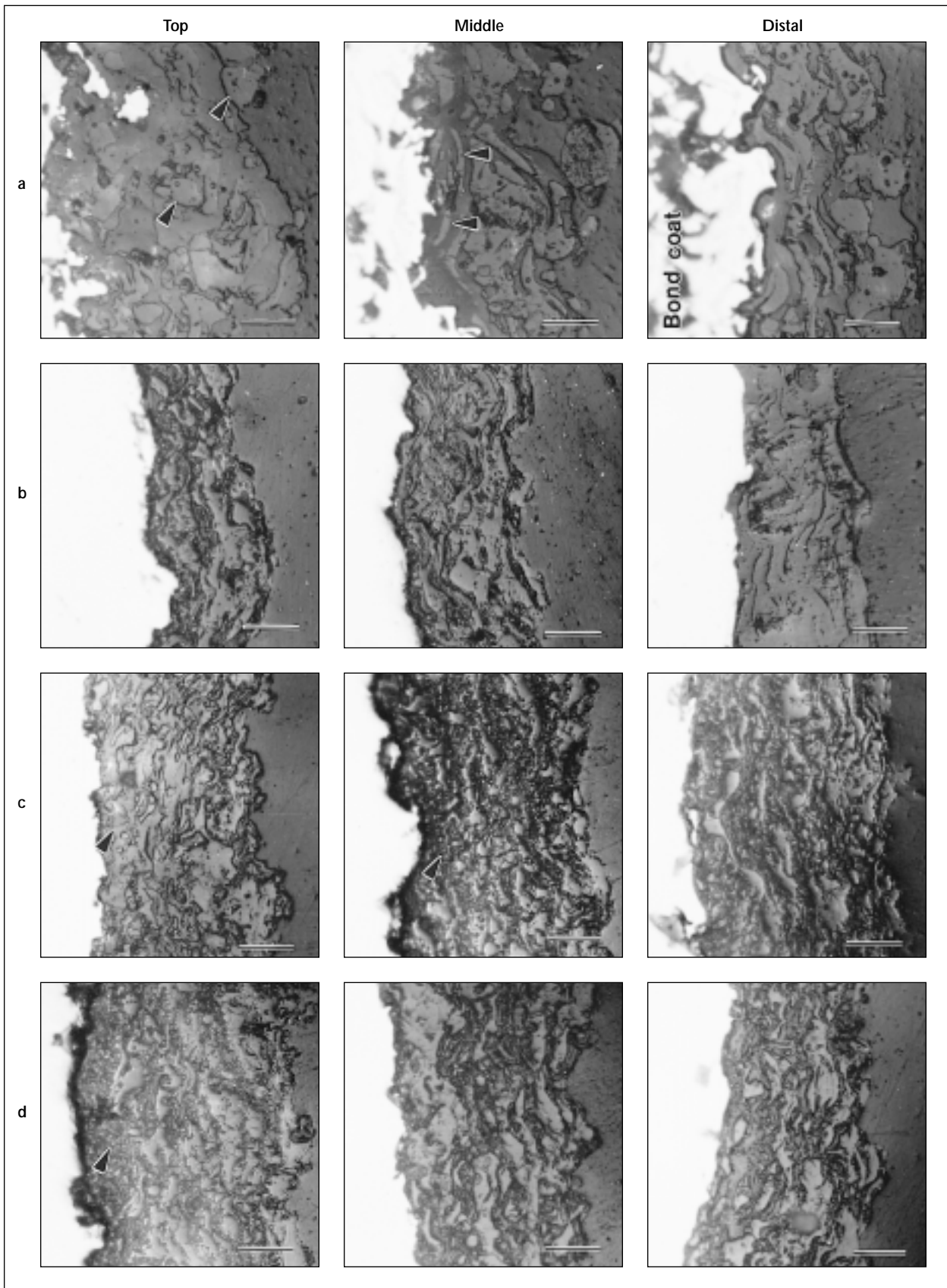


**Fig 3** Four press-fit implants (a to d), illustrating the coating microstructure of the top, middle, and distal locations of the implant. The magnification marker represents 20  $\mu\text{m}$ . The metallic implant is identified by the white area to the left, followed by the coating in the middle, and the epoxy resin to the right. *Arrowheads* in the top of the implant show partially molten particles in a, an amorphous phase in c, and a recrystallized area in d. *Arrowheads* in the middle of the implant illustrate crystalline lamellae in a and a recrystallized region in c.

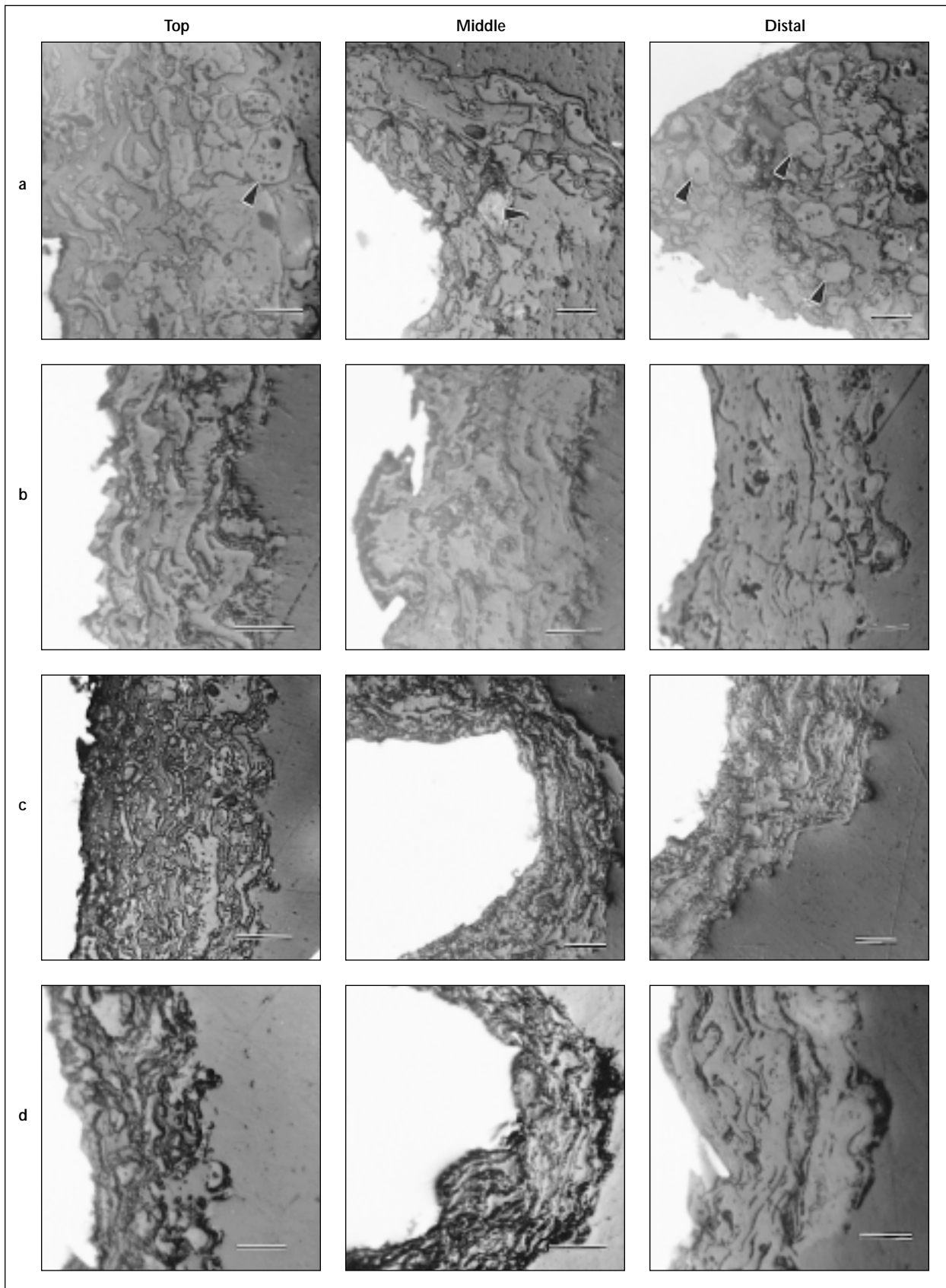


**Fig 4** Coating microstructure of four threaded implants (a to d). The metallic implant is identified by the white area to the left, followed by the coating in the middle, and the epoxy resin to the right. The regions in the coating marked with an *arrowhead* are crystalline regions referred to in the text. The microstructure of the distal location of Fig 4a represents the gully of a thread and not the distal location. A magnification marker represents a length of 20  $\mu\text{m}$ . Micrographs show the entire tip of the thread and therefore have a smaller magnification.

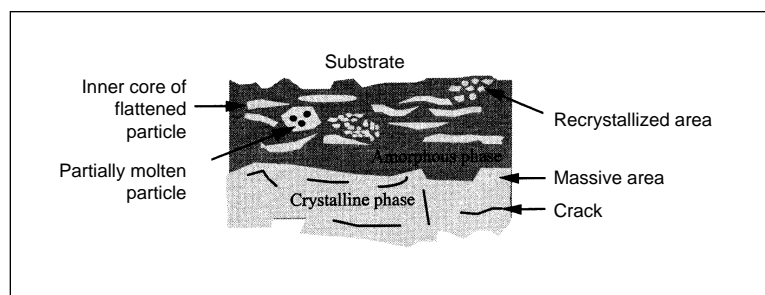


**Fig 5** A cross section revealing an amorphous phase (darker grey) and the various forms of crystalline phase (lighter grey) in a possible coating assembly.

**Table 1** Microstructural Aspects of the Hydroxyapatite Coatings

Implant label	Crystallinity (%)	Major crystalline form	Crystallinity gradient	Thickness ( $\mu\text{m}$ )
3a	40–60	Partially molten, lamellar	—	30–75
3b	80–100	Lamellar, recrystallized, massive	Sagittally	30–50
3c	85–95	Lamellar, recrystallized	Thickness	80–100
3d	80–90	Lamellar, recrystallized	—	60–90
4a	50–75	Partially molten, lamellar, massive	Thickness, thread tip	30–75
4b	80–100	Lamellar, massive	Sagittally	50–75
4c	70–80	Lamellar, recrystallized	—	40–75
4d	70–100	Partially molten, lamellar, massive	Sagittally	40–60

talline phase appeared to be located away from the substrate, either randomly distributed throughout the collar region or within the center of the coating in regions near the middle of the implant. An amorphous layer is positioned adjacent to the substrate for both cross sections.

The distal area (Fig 3a) displayed more crystalline material, about 60%. Again, an amorphous layer lined the substrate, followed by elongated crystallized regions of molten droplets. The rounded shape of the crystalline islands with the contained porosity, located toward the outside of the coating, was representative of the powder used for spraying and suggests that some of the powder received insufficient heat input during transport through the plasma flame.

A variation in crystalline phase content with coating location was also apparent in other implants (Figs 3b, 4b, and 4d). Crystallinity increased from 80 wt% (Fig 3b) and 75 wt% (Fig 4b) in the collar region to 100% distally. The powder used to produce this coating was totally molten, as was revealed by the elongated shape of the crystalline segments close to the substrate both in the collar and middle implant areas.

Small crystallized islands, less than 2  $\mu\text{m}$  in size, were found between the larger crystalline areas. Identification of the individual features was more complicated in these coatings. This was most prevalent in the middle and distal coating of Fig 3c and in

the top coating of Fig 3d. The microcrystalline region was visible in those regions that would have otherwise been occupied by the amorphous phase. For example, the area adjacent to the substrate in the collar of the implant in Fig 3c was occupied by the amorphous phase, but further down the implant, small crystallized areas filled the area between the larger crystalline segments. The implant in Fig 3d depicted this microstructure in the collar portion.

The crystallinity in the first half of the coating thickness at the top of the implant in Fig 4a was 40 wt%, but the external surface displayed a 75 wt% crystalline content where large crystalline regions dominated. The overall crystalline content was about 55 wt%. Analysis of this implant surface with conventional x-ray diffraction would not reveal this depth dependency.

A higher crystalline content can be observed on the tip of the thread (Fig 4a). The top area of the thread, however, had a distinct area of amorphous phase. The root of the thread was filled with partially molten particles.

Figure 4c displayed an even coating on the threads and exhibited a microstructure consisting of predominantly smaller crystalline regions. Other implants with this feature included those in Figs 3c and 3d. Table 1 summarizes the characteristics of the crystalline phases detected in the coatings.

## Discussion

**Substrate Roughness, Coating Thickness, and Coating Surface Assessment.** Substrate surface roughness can lead to unevenness in thin coatings; however, surface roughness is an essential processing requirement to enhance coating adhesion.<sup>29</sup> Molten particles during the coating stage impact and flow around the jagged asperities of the prepared surface, thus producing an interlocking effect. This is the main mechanism for attachment of thermally sprayed coatings. The intermediate layer used in a press-fit type of implant (Fig 3a), provided as a bond coat, produced an increased apparent roughness. This design of implant coating allows dissolution followed by bone growth into the porous substrate. In the event of coating dissolution, the bone may then grow into the roughened surfaces and establish a mechanical interlock.

One aspect of variability in the implants, which is not an issue for machined surfaces, is the unevenness of the implant surface. This unevenness is created either by the use of a thin coating on a rough substrate (Fig 3b), by the presence of partially molten particles on the surface of a coating (Fig 3a), or by local thickness variations of coatings on threads (Fig 4a). Placement of these coatings in a prepared site would produce only isolated areas in contact with the osseous tissue. These surface variations may also affect the ease of implant placement into a tapped osteotomy site. A nonuniform coating (see Figs 3a and 4a) may require a larger force for implant placement, thereby subjecting the coating to higher forces and modifying the bone bed. Mechanical deformation of the bone could decrease bone apposition and interface strength in sites of higher bone density.<sup>30</sup>

Studies on the surface integrity of several hydroxyapatite coatings after implant placement indicate that some defragmentation of areas may occur.<sup>31</sup> Particles on the outer surface could also be removed if not well attached, as in cases of high surface roughness. A rough coating can be imparted when unmolten or partially molten particles are transferred to the coating during the deposition process. These appear as lightly shaded round particles, about 10 to 30  $\mu\text{m}$  in size, in Figs 3a and 4a.

Coating uniformity is particularly important when the implant coating is designed to be slightly porous so as to contain bone morphogenic proteins or drugs to assist the healing process.<sup>32,33</sup> Surgical drills must thus closely replicate the contours of the outer body to prevent coating damage and unnecessary trauma to the bone. Alternatively, sites may be drilled slightly larger, allowing osteoconductivity of calcium phos-

phates to bridge the gap. A new advance in coating design avoids the use of coating on the distal location, thus preventing coating delamination from the implant placed into the dense bone.

**Crystallinity in Hydroxyapatite Coatings.** Areas adjacent to the substrate are typically covered with an amorphous phase, because of the very fast cooling rate on the metal surface.<sup>34</sup> Slower heat dissipation through the previously deposited layer produces a slower cooling rate for crystallization of part of the deposited molten droplet. This crystalline area, which represents the building block of thermally sprayed coatings, appears as long flattened particles that can be identified in most of the implants. When the initial particle size used for spraying has been very small, the lenticular shapes may be more difficult to identify (Fig 3c).

Increasing coating temperature during the spraying process to between 500 and 700°C produces crystallization.<sup>35</sup> Crystallization can occur as heat is transported through a previously deposited amorphous region during the spraying process. Recrystallization then occurs, producing microcrystalline areas that grow after the passage of heat and may result in microcrystalline areas or massive areas. The buildup of heat will be dictated by the capacity of the implant to dissipate the heat. This is evident in those locations of the implant where heat dissipation is the slowest, such as the distal end (Figs 3b, 4b, and 4d) or the thread tip (Fig 4a). The apical hole used in some implant designs, which supposedly offers advantages in implant stabilization, decreases the thermal mass and thus increases the likelihood of crystallization at the tip of the implant from heat buildup. Recrystallization may also be observed on a smaller scale. The area adjacent to the substrate in the top of the implant is amorphous, whereas recrystallized regions are already observed lower on the implant. Comparison with the small crystallized areas at the collar portion (Fig 3d) suggests that more heat was available at the top of the implant. Large areas of crystallized material are typically associated with cracks. These form as a response to anisotropic contraction within the coating during crystallization.<sup>35</sup> Cracks are an intrinsic part of thermally sprayed coatings<sup>36</sup> and should only be a concern when they become large or are interconnected. Reports of other coatings have also revealed cracks.<sup>37</sup>

Coating temperature may vary within the coating thickness in addition to implant location. The low thermal conductivity of hydroxyapatite suggests that the temperature is likely to reach higher levels on the external surface of the coating. An example of a crystalline gradient may be seen in the top area of the implant in Fig 4a. Threads on screw-type implants

are sites where the buildup of heat can produce massive crystallization. Figure 4a shows that the front face of the thread, which was subjected to the heat from the thermal spray torch, has produced a higher crystalline content, whereas the other side of the thread has experienced a shadow effect and contains more amorphous phase.

The cross section of other implants in the literature<sup>38,39</sup> also revealed microstructures and coating thickness variations comparable to those reported here. Another microstructural feature is coating porosity. Most of the visible porosity in the implants, identified as small black dots, has been isolated to the partially molten powders or to large crystalline areas.

Location of the amorphous phase is dictated collectively, by (1) the cooling rate of the molten droplet, (2) the temperature of the coating, and (3) the chemical composition of the melt.<sup>40</sup> The microstructures of coatings have indicated that the amorphous phase usually surrounds crystalline regions and is more dominant at the substrate as opposed to the outer surface of the coating.

The occurrence of the amorphous phase is determined by factors that include powder feedstock, spraying parameters, and implant design. The small particle size used for producing thin and even coatings on dental implants has generally produced higher crystallinity coatings by minimizing the heat transfer to the powder. The steep angled surface on some of the threaded dental implants causes more droplet spreading as is favorable for forming the amorphous phase. Coating parameters and implant design collectively determine the nature of the coating. The plasma-spraying process can be controlled to produce a coating with the desired crystalline phase content (up to 100%), thus avoiding posttreatment alternatives to increase the crystalline content. The substrate temperature, which does not appear to have been intentionally controlled in the examined coatings, can facilitate a high crystallinity coating when used above the crystallization temperature. Other methods of avoiding the amorphous phase are presently being investigated.

#### **Evaluation of Hydroxyapatite Coatings.**

Previous work has illustrated the preferred dissolution of the amorphous phase.<sup>41</sup> Calcium phosphates that are resorbed more quickly, both chemically and cellularly, are accompanied by faster bone formation around the implant.<sup>42</sup> This faster healing accompanied by better initial stabilization<sup>43</sup> could decrease the time for osseointegration. However, the integrity of the implant may suffer depending on its microstructure. Histology of the tissue adjacent to hydroxyapatite coatings has revealed loose particles, which have been found in the surrounding tis-

sue.<sup>20,44-46</sup> Larger fragments separated from the tip of threads on screw-type implants have been detected.<sup>47</sup> Analogy to Fig 4b suggests that the massive crystalline region can be dislodged by preferred dissolution of the amorphous phase. The action of higher stress levels on the tip of implants,<sup>48</sup> in conjunction with process-induced stresses,<sup>49</sup> can accelerate the amorphous phase dissolution. Coatings with an amorphous phase at the interface may produce a weaker substrate-coating interface<sup>21</sup> over time, which could lead to delamination.<sup>17,50</sup> The preferred microstructure of those implants examined is the microcrystalline coating observed in Fig 3c, which would degrade slowly and uniformly.

The requirements of a placed implant are for it to be stabilized by the growth of bone up to the implant and for the epithelium to attach firmly to the neck so as to isolate the underlying connective tissue and bone. The coating material in this location must be stable to avoid rapid coating destruction through infection. The implants analyzed here contain an amorphous phase within this location. Oral cleanliness and plaque control are very important to implant survival.

Issues such as the amorphous phase content and the distribution and size of crystalline regions must be considered in implant design. Despite the controversy concerning the benefit of hydroxyapatite coatings,<sup>51-55</sup> clinical studies have reported high success rates.<sup>8,10,56,57</sup> Improvements in the coating quality will continue to provide high attachment strength and a more predictable long-term coating performance, especially with press-fit implants.<sup>58-60</sup>

#### **Conclusion**

An examination of various commercial implants revealed that all hydroxyapatite coatings are not identical. An increase in crystalline content can occur with thickness toward the apical end of the implant and on the tips of threads. Crystalline segments vary from micrometer-sized areas up to the entire coating thickness, depending on the mechanism of formation. The different crystallinity of coatings with variable crystalline segment sizes and location suggests that coating performance can be predicted based on the coating microstructures.

#### **Acknowledgments**

Karlis Gross was supported by an Australian Research Council award during the preparation of this manuscript. Christopher C. Berndt acknowledges support from MRSEC Program DMR 9632570. This study is a part of the research reported in a doctoral dissertation, "The Amorphous Phases in Hydroxyapatite Coatings," conducted at the State University of New York at Stony Brook.

## References

1. McKinney RV. *Endosteal Dental Implants*. St Louis: Mosby Year Book, 1991.
2. Schulte W, Heimke G. The Tübingen immediate implant. *Quintessenz* 1976;6:17–23.
3. Gomez-Roman G, Schulte W, d'Hoedt B, Axman-Krcmar D. The Frialit-2 implant system: Five-year clinical experience in single-tooth and immediately postextraction applications. *Int J Oral Maxillofac Implants* 1997;12:299–309.
4. DePorter DA, Watson PA, Pilliar RM, Chipman ML, Valiquette N. A histological comparison in the dog of porous coated vs. threaded dental implants. *J Dent Res* 1990;69:1138–1145.
5. Block MS, Finger IM, Fontenot MG, Kent JN. Loaded hydroxylapatite coated and grit blasted titanium implants in dogs. *Int J Oral Maxillofac Implants* 1989;4:219–225.
6. Albrektsson T. Implant biocompatibility. In: *The 3rd International Symposium on Titanium in Dentistry*. Sydney: Univ of Sydney, 1995.
7. Leimola-Virtanen R, Peltola J, Oksala E, Helenius H, Happonen RP. ITI titanium plasma-sprayed screw implants in the treatment of edentulous mandibles: A follow-up study of 39 implants. *Int J Oral Maxillofac Implants* 1995;10:373–378.
8. Wheeler SL. Eight-year clinical retrospective study of plasma-sprayed and hydroxyapatite-coated cylinder implants. *Int J Oral Maxillofac Implants* 1996;11:340–350.
9. Kay JF, Jarcho M, Logan G, Embry J, Stinnes C. Physical and chemical characteristics of hydroxylapatite coating on metal [abstract 472]. *J Dent Res* 1986;65:222.
10. Kent J, Block M, Finger I, Guerra L, Larsen, Misiek D. Biointegrated hydroxylapatite-coated dental implants: 5-year clinical observations. *J Am Dent Assoc* 1990;121:138–144.
11. Geesink RGT, Hoefnagels NHM. Six-year results of hydroxyapatite-coated total hip replacement. *J Bone Joint Surg (Br)* 1995;77:534–547.
12. Soballe K, Hansen ES, Brockstedt-Rasmussen H, Bünger C. Migration of hydroxyapatite coated femoral prosthesis. *J Bone Joint Surg (Br)* 1993;75:681–687.
13. Lozada JL, James RA and Boskovic M. HA coated implants: Warranted or not? *Compend Contin Educ Dent* 1993;14(suppl 15):539–543.
14. Knox R, Lee K, Meffert R. Placement of hydroxyapatite-coated endosseous implants in fresh extraction sites: A case report. *Int J Periodont Rest Dent* 1993;13:243–253.
15. Lum LB, Beirne DR, Curtis DA. Histologic evaluation of hydroxylapatite-coated versus uncoated titanium blade implants in delayed and immediately loaded applications. *Int J Oral Maxillofac Implants* 1991;6:456–462.
16. Misch CM. Hydroxylapatite-coated implants. Design considerations and clinical parameters. *NY State Dent J* 1993;5:36–41.
17. Cook S, Salkeld S, Gaisser D, Wagner W. The effect of surface macrotexture on the mechanical and histologic characteristics of hydroxyapatite-coated dental implants. *J Oral Implantol* 1993;19:288–294.
18. David A, Eitenmuller J, Muhr G, Pommer A, Bar HF, Ostermann PA, et al. Mechanical and histological evaluation of hydroxyapatite-coated, titanium-coated and grit-blasted surfaces under weight-bearing conditions. *Arch Orthop Trauma Surg* 1995;114:112–118.
19. Strunz V, Schmitz HJ, Fritz R, Fuhrman G, Gross U. Shear strength and tensile strength. A comparison of titanium plasma flame-sprayed and hydroxyapatite coated IMZ implants. *Z Zahnartztl Implantol* 1988;4:139–144.
20. Benjamin LS, Block MS. Histologic evaluation of a retrieved human HA-coated subperiosteal implant: Report of a case. *Int J Oral Maxillofac Implants* 1989;4:63–66.
21. Denissen HW, Kalk W, deNieuport HM, Maltha JC, van de Hoof A. Mandibular bone response to plasma-sprayed coatings of hydroxyapatite. *Int J Prosthodont* 1990;3:53–58.
22. Wennerberg A, Albrektsson T, Andersson B. Design and surface characteristics of 13 commercially available oral implant systems. *Int J Oral Maxillofac Implants* 1993;8:622–633.
23. Quirynen M, Bollen CML, Willems G, van Steenberghe D. Comparison of surface characteristics of six commercially pure titanium abutments. *Int J Oral Maxillofac Implants* 1994;9:71–76.
24. Dalton JE, Cook SD. In vivo mechanical and histological characteristics of HA-coated implants vary with coating vendor. *J Biomed Mater Res* 1995;29:239–245.
25. Krauser JT. X-ray diffraction analysis of hydroxylapatite-coated implants. *Int J Oral Maxillofac Implants* 1997;7:124–125.
26. Glick P, Versman K. To minimize complications, is it essential that implant abutments be surrounded by keratinized tissue [current issues forum]? *Int J Oral Maxillofac Implants* 1997;12:128–129.
27. Kingery WD, Bowen HK, Uhlmann DR. *Introduction to Ceramics*, ed 2. New York: John Wiley and Sons, 1976:654–661.
28. ASTM. Standard specification for composition of ceramic hydroxylapatite for surgical implants. ASTM 1993;F1185–1188:456–457.
29. Berndt CC, Lin CK. Measurement of adhesion for thermally sprayed materials. *J Adhesion Sci Tech* 1993;7:1235–1264.
30. Tanaka M, Sawaki Y, Niimi A, Kaneda T. Effects of bone tapping on osseointegration of screw dental implants. *Int J Oral Maxillofac Implants* 1994;9:541–547.
31. Edmonds RM, Yukna RA, Moses RL. Evaluation of the surface integrity of hydroxyapatite coated threaded dental implants after insertion. *Implant Dent* 1996;5:273–278.
32. Denissen H, van Beek E, Lowik C, Papapoulos S, van den Hooff A. Ceramic hydroxyapatite implants for the release of biphosphonate. *Bone Miner* 1994;25:123–134.
33. Radin S, Campbell JT, Ducheyne P, Cuckler JM. Calcium phosphate ceramic coatings as carriers of vancomycin. *Biomaterials* 1997;18:777–782.
34. Gross KA, Berndt CC, Herman H. The amorphous phase formation in plasma sprayed hydroxyapatite coatings. *J Biomed Mater Res* 1998;39:407–414.
35. Gross KA, Gross V, Berndt CC. Thermal analysis of the amorphous phase in plasma sprayed hydroxyapatite coatings. *J Am Ceram Soc* 1998;81:106–112.
36. Ilavsky J, Allen AJ, Long GG, Kreuger S, Berndt CC, Herman H. Influence of spray angle on the pore and crack microstructure of plasma-sprayed deposits. *J Am Ceram Soc* 1997;80:733–742.
37. Kim Y, LeGeros J, LeGeros R. Characterization of commercial HA-coated dental implants [abstract 287]. *J Dent Res* 1994;73:137.
38. Tufeci E, Brantley WA, Mitchel JC, McGlumphy EA. Microstructures of plasma sprayed hydroxyapatite-coated Ti-6Al-4V dental implants. *Int J Oral Maxillofac Implants* 1997;12:17–24.
39. Hemmerté J, Öncag A, Ertürk S. Ultrastructural features of the bone response to a plasma-sprayed hydroxyapatite coating in sheep. *J Biomed Mater Res* 1997;36:418–425.
40. Gross KA. *The Amorphous Phases in Hydroxyapatite Coatings* [thesis]. Stony Brook, NY: SUNY at Stony Brook, 1995.

41. Gross KA, Berndt CC, Goldschlag DD, Iacono VJ. In vitro changes of hydroxyapatite coatings. *Int J Oral Maxillofac Implants* 1997;12:589-597.
42. Barney VC, Levin MP, Adams DF. Bioceramic implants in surgical periodontal defects—A comparison study. *J Periodontol* 1986;57:764-771.
43. Huracek J, Spirig P. The effect of hydroxyapatite coating on the fixation of hip prostheses. A comparison of clinical and radiographic results of hip replacement in a matched-pair study. *Arch Orthop Trauma Surg* 1994;113:72-77.
44. Lintner F, Bohm G, Huber M, Scholz R. Histology of tissue adjacent to an HAC-coated femoral prosthesis. A case report. *J Bone Joint Surg (Br)* 1994;76:824-830.
45. Takeshita F, Ayukawa Y, Iyama S, Suetsugu T, Kido MA. A histologic evaluation of retrieved hydroxyapatite-coated blade-form implants using scanning electron, light, and confocal laser scanning microscopies. *J Periodontol* 1996;67:1034-1040.
46. Yang CY, Wang BC, Lee TM, Chang E, Chang GL. Intramedullary implant of plasma-sprayed hydroxyapatite coating: An interface study. *J Biomed Mater Res* 1997;36:39-48.
47. Gottlander M, Albrektsson T. Histomorphometric analysis of hydroxyapatite-coated and uncoated titanium implants. The importance of implant design. *Clin Oral Implants Res* 1992;3:71-76.
48. Ben-Nissan B, Bodur CT, Lutton P. Biomechanical Optimisation of Dental Implants with Finite Element Analysis. Proceedings of Australian Society for Biomaterials 4th Annual Conference. Sydney, 1994:40.
49. Sergio V, Sbaizero O, Clarke DR. Mechanical and chemical consequences of the residual stresses in plasma sprayed hydroxyapatite coatings. *Biomaterials* 1997;18:477-482.
50. Nimb L, Gotfredsen K, Steen JJ. Mechanical failure of hydroxyapatite-coated titanium and cobalt-chromium-molybdenum alloy implants. An animal study. *Acta Orthop Belg* 1993;59:333-338.
51. Hurson S. Differentiation of HA coatings. *J Dent Symp* 1993;1:65-66.
52. Kwan JY. HA coatings in implant dentistry—hype, hysteria, and clinical reality. *Implant Soc* 1993;3:16.
53. Morscher EW. Hydroxyapatite coating of prostheses [editorial]. *J Bone Joint Surg [Br]* 1991;73:705-706.
54. Zablotzky M. HA coatings in implant dentistry: Hype, hysteria, or clinical reality? *J Dent Symp* 1993;1:70-72.
55. Kay JF. Calcium phosphate coatings: Understanding the chemistry and biology and their effective use. *Compend Contin Educ Dent* 1993;4(suppl 15):520-525.
56. Lozada JL. Eight-year clinical evaluation of HA-coated implants. *J Dent Symp* 1993;1:67-69.
57. Fettig RH, Kay JF. A seven-year clinical evaluation of soft-tissue effects of hydroxylapatite-coated vs. uncoated subperiosteal implants. *J Oral Implantol* 1994;20:42-48.
58. Gottlander M, Albrektsson T, Carlsson LV. A histomorphometric study of unthreaded hydroxyapatite-coated and titanium-coated implants in rabbit bone. *Int J Oral Maxillofac Implants* 1992;7:485-490.
59. Weinlander M, Kenney EB, Lekovic V, Beumer J, Moy PK, Lewis S. Histomorphometry of bone apposition around three types of endosseous dental implants. *Int J Oral Maxillofac Implants* 1992;7:485-490.
60. Clemens JAM, Klein CPAT, Sackers RJB, Dhert WJA, de Groot K, Rozig PM. Healing of gaps around calcium phosphate-coated implants in trabecular bone of the goat. *J Biomed Mater Res* 1997;36:55-67.